

## X-ray Emission from Gigahertz Peaked/Compact Steep Spectrum Sources

Aneta Siemiginowska<sup>1</sup>, Thomas L. Aldcroft<sup>1</sup>, Jill Bechtold<sup>2</sup>,  
Gianfranco Brunetti<sup>3</sup>, Martin Elvis<sup>1</sup> and Carlo Stanghellini<sup>4</sup>

<sup>1</sup> Harvard–Smithsonian Center for Astrophysics, 60 Garden St., Cambridge, MA 02138, USA  
asiemiginowska@cfa.harvard.edu

<sup>2</sup> Steward Observatory, University of Arizona, Tucson AZ 85721, USA

<sup>3</sup> Istituto di Radioastronomia del CNR, Via Gobetti 101, 40129 Bologna, Italy

<sup>4</sup> Istituto di Radioastronomia del CNR, Contrada Renna Bassa, 96017 Noto, Italy

Received 2002 July 20, accepted 2003 March 01

**Abstract:** The high spatial resolution of the *Chandra* X-ray Observatory allows us to study the environment of GPS/CSS sources to within an arcsec of the strong compact core. We present the discovery of X-ray jets in two GPS quasars, PKS1127–145 and B2 0738+313, indicating that X-ray emission associated with the relativistic plasma is present at large distances from the GPS nucleus. We also discuss first results from *Chandra* observations of our GPS/CSS sample. We find that six out of ten sources show intrinsic absorption at a level which may be sufficient to confine the GPS source.

**Keywords:** galaxies: active — X-rays: galaxies

### 1 Introduction

Gigahertz peaked spectrum (GPS) and compact steep spectrum (CSS) sources are major classes of radio sources which may offer glimpses of the early stages of radio source formation. They could well offer insight into the physical processes triggering activity in galactic nuclei and so into the causes of quasar evolution. Although these sources are now receiving considerable attention in the radio band, they remain neglected at other wavelengths.

During the last two decades there has been *no* systematic X-ray study of GPS/CSS sources and only a few X-ray observations have been performed. O’Dea (1998) lists 31 sources with available X-ray information, including seven sources with upper limits only. This sample shows, as expected, that galaxies are less luminous than quasars in X-rays. Elvis et al. (1994) observed X-ray absorption in two out of three high redshift GPS quasars, suggesting that their environment might be different from other quasars. ROSAT upper limits for a few GPS/CSS galaxies of  $L_x < 3 \times 10^{42} \text{ erg s}^{-1}$  are consistent with the X-ray emission expected from poor clusters or early type galaxies. O’Dea et al. (2000) presented the first X-ray detection of a GPS galaxy, which had  $L_x \sim 2 \times 10^{42} \text{ erg s}^{-1}$  with ASCA. Before *Chandra*, observations at the highest spatial resolution were made with the ROSAT HRI in which two out of four GPS quasars showed traces of extended emission (Antonelli & Fiore 1997).

The lack of available X-ray information is surprising, since strong X-ray emission is expected to be associated with strong radio power. In principle such information could help in understanding the emission processes and dynamics related to radio-emitting structures, and help in answering the question, is the X-ray emission directly connected to the expanding jet? X-ray emission associated with a local halo or cluster ( $T \sim 10^7 \text{ K}$ ) could also help

in studying the environment of GPS/CSS sources, and we should be able to look for the remnants of a merger event or signatures of interactions between an expanding radio plasma and the IGM. In addition X-ray spectra can constrain the total absorbing column, thus we may be able to check whether there is sufficient material to confine the GPS source.

X-rays can also help us understand any link between GPS and large scale radio sources and answer questions related to the source evolution such as: Can we see any evidence for intermittent activity? Do GPS sources grow into large radio galaxies?

The *Chandra* X-ray Observatory, with its exceptional image quality (PSF FWHM of  $\sim 0.5 \text{ arcsec}$ ), has discovered many X-ray jets associated with radio structures in radio galaxies and quasars (see <http://hea-www.harvard.edu/XJET/>). *Chandra* is the only X-ray telescope which can resolve structures on 1 arcsec scales, and is well-suited for studying the environment of GPS/CSS sources. Observations made with *Chandra* could determine whether X-ray jets are present in GPS sources and whether extended emission hinted at in ROSAT HRI images is indeed present in two GPS quasars.

Here, we present *Chandra* observations of two GPS sources, PKS 1127–145 and B2 0738+313, in which we have discovered X-ray jets. We also present preliminary analysis of our GPS/CSS sample observed during the first half year of the *Chandra* AO3 cycle.

We assume  $H_0 = 50 \text{ km s}^{-1} \text{ Mpc}^{-1}$  and  $q_0 = 0.5$ .

### 2 Observations of PKS 1127–45 and B2 0738+313

#### 2.1 Source Properties

We observed the two GPS quasars with the *Chandra* ACIS-S detector. PKS 1127–45 is a quasar at  $z = 1.187$  with  $L_{\text{bol}} = 5 \times 10^{46} \text{ erg s}^{-1}$  and a GPS radio spectrum

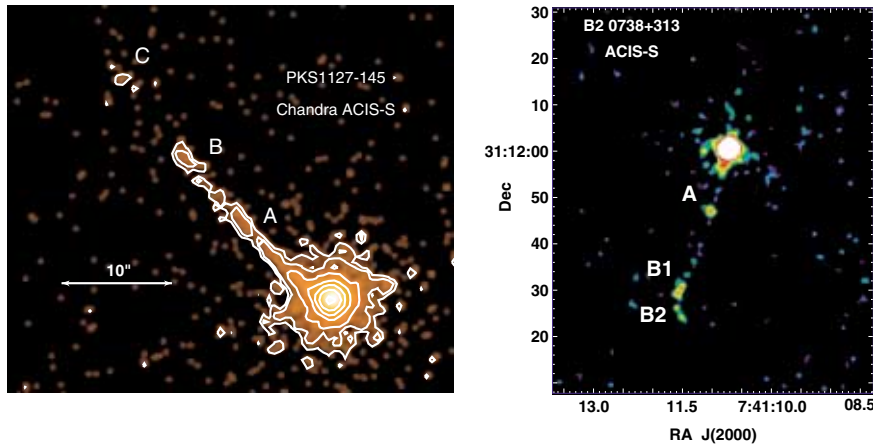


**Figure 1** *Chandra* ACIS-S images smoothed with a Gaussian kernel (FWHM = 0.75 arcsec). Only the photons with energies between 0.3–6 keV have been included in the image. North is up and east is to the left. (a) PKS 1127–145. The knots are labelled A, B, C. Contour levels: 1.2, 2.6, 4.5, 9, 27, 3000 counts pixel<sup>-1</sup> (Siemiginowska et al. 2002a). (b) B2 0738+313. The jet components, A, B1 and B2 are indicated in the figure. The peak emission at the core corresponds to  $4.5 \times 10^{-7}$  photons cm<sup>-2</sup> s<sup>-1</sup> pixel<sup>-1</sup> (1 pixel = 0.164 arcsec) (Siemiginowska et al. 2002b).

that peaks at  $\sim 1$  GHz. It also has an intervening damped Lyman- $\alpha$  system (DLA) at  $z_{\text{abs}} = 0.312$  (Bechtold et al. 2002). The *Chandra* ACIS-S observation shows a  $\sim 30$  arcsec X-ray jet; at the quasar redshift it is  $\sim 330 h_{50}^{-1}$  kpc projected on the sky (Fig. 1). As described in Siemiginowska et al. (2002a), the jet curves and its emission is very faint in comparison to the nucleus. The ratio of the intensity of individual knots to the core intensity is  $\sim 1 : 450$ . There is only rough correspondence between the X-ray knots and the VLA knots, with X-ray peak intensities preceding the radio peak intensities. The X-ray emission is stronger at the core, while the radio emission is stronger away from the core.

B2 0738+313 is a quasar at  $z = 0.63$  and  $L_{\text{bol}} \sim 10^{46}$  erg s<sup>-1</sup>. It has two DLA systems at  $z = 0.0912$  and  $0.2212$  (Rao & Turnshek 1998). The GPS radio spectrum peaks at  $\sim 5$  GHz (Stanghellini et al. 1998). ROSAT HRI observations show a hint of the extended emission present on 10–20 arcsec scales. With a 27 ksec *Chandra* ACIS-S observation we detected an X-ray jet extending up to  $\sim 35$  arcsec away from the nucleus, with a few enhancements in the form of hot spots and knots (Figure 1). The hot spot emission is faint compared to the core, with an intensity ratio of  $\sim 1 : 200$ . VLA radio maps show faint extended radio emission in the form of lobes to the north and south. The X-ray jet follows the radio emission to the south (Figure 2). The X-ray jet emission becomes fainter moving away from the core, while the radio emission has two hot spots at the end of the southern lobe. There is NO X-ray emission corresponding to the northern radio lobe with a  $3\sigma$  upper limit of  $2 \times 10^{-9}$  photons cm<sup>-2</sup> s<sup>-1</sup> pixel<sup>-1</sup> (1 pixel = 0.164 arcsec).

## 2.2 Jet Emission Models

Comparison of X-ray, optical and radio data rules out thermal emission, synchrotron self-Compton (SSC) and simple direct synchrotron emission (see Harris &

Krawczynski 2002 for review) as the origin of the X-ray jet emission in PKS 1127–45. Inverse Compton scattering off cosmic microwave background photons (EIC/CMB) with moderate jet bulk velocities ( $\Gamma_{\text{bulk}} \sim 2\text{--}3$ ) can readily accommodate the observations because the EIC/CMB process is especially effective at high redshift due to the  $(1+z)^4$  scaling of the CMB. We note that X-rays from EIC can trace the low energy ( $\gamma \leq 10^3$ ) population of particles which are not detectable in the radio band and thus delineate the ‘fossil’ structure.

The X-ray emission in the two knots (B1, B2) of the B2 0738+313 jet can be explained by synchrotron emission. However, knot A needs an additional component, because synchrotron emission requires unusually high acceleration efficiencies. Note that in the synchrotron model the high energy break needs to be at  $\nu > 10^{19}$  Hz, which seems unlikely. The EIC/CMB process requires  $\Gamma_{\text{bulk}}$  of  $\sim 10$  (Fig. 2) and might be a possible explanation for the knot A X-ray emission.

## 2.3 Summary

Our observations lead us to conclude that:

- X-ray jets in both sources extend far away from the nucleus,  $\sim 300$  kpc projected distance.
- X-ray emission is most likely due to the interactions between relativistic jet particles and CMB photons.
- X-ray jet emission indicates the presence of relativistic motion up to a distance of several hundred kpc from the nucleus:  $\Gamma_{\text{bulk}} \sim 3\text{--}10$ .

## 3 The First X-ray GPS/CSS Sample Observed with *Chandra*

The discovery of two X-ray jets associated with GPS quasars raises more questions about the nature of GPS sources: Are GPS/CSS sources truly compact or do they have extended structures, and are these structures too faint

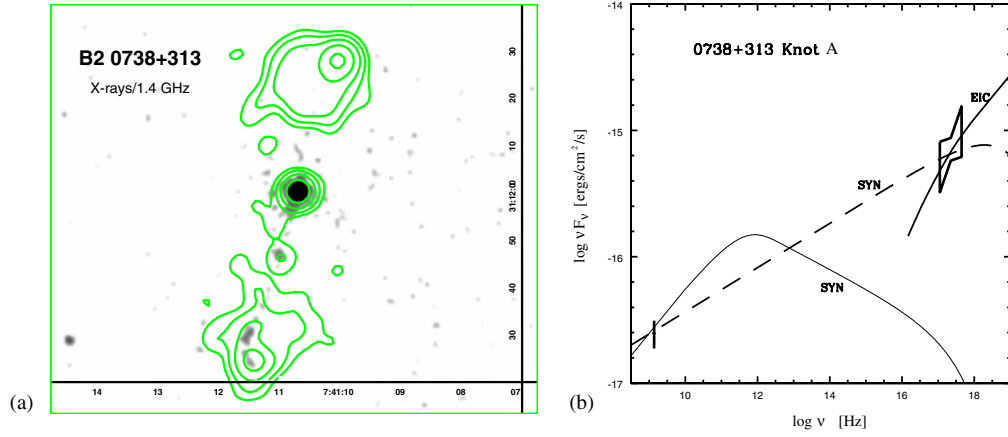


**Figure 2** (a) Superposition of B2 0738+313 *Chandra* X-ray image (grey) with the radio (1.4 GHz) contours. The strong radio core has been partly subtracted. Contour peak radio flux is at  $1.47 \times 10^{-2} \text{ Jy beam}^{-1}$  and contour levels are  $2.5 \times 10^{-4}$  (−3, 3, 6, 12, 25, 50). Grey scale in the X-ray image (0.3–6 keV) varies from  $10^{-7}$  to  $5 \times 10^{-7} \text{ photons cm}^{-2} \text{ s}^{-1} \text{ pixel}^{-1}$  (1 pixel = 0.164 arcsec). North is up and east is to the left. (b) B2 0738+313: Jet emission models for knot A. The dashed line shows the synchrotron model with required high energy cut-off of greater than  $10^{19} \text{ Hz}$ . The solid line shows the Inverse Compton model with the CMB being a source of external photons:  $\alpha = 0.5\text{--}0.6$ ,  $\Gamma_{\text{bulk}} = 10$ ,  $\theta < 5^\circ$ ,  $B = 15 \mu\text{G}$ . Data points in radio and X-rays are shown.

**Table 1.** GPS/CSS *Chandra* Sample

Name	Redshift	$(N_{\text{H}})^a$ $\text{E20 cm}^{-2}$	$(N_{\text{H}}^{\text{zabs}})^b$ $\text{E21 cm}^{-2}$	$\Gamma^c$	$f_{(0.1-2 \text{ keV})}^d$ $\text{erg cm}^{-2} \text{ s}^{-1}$	$f_{(2-10 \text{ keV})}$ $\text{erg cm}^{-2} \text{ s}^{-1}$
0941–080	0.228	3.67	–	$1.50 \pm 2.40$	$3.10 \times 10^{-15}$	$7.10 \times 10^{-15}$
0134+329	0.367	4.54	<2.1	$1.96 \pm 0.04$	$1.82 \times 10^{-12}$	$2.20 \times 10^{-12}$
B2 0738+313	0.63	4.18	$2.1 \pm 0.3$	$1.56 \pm 0.05$	$2.98 \times 10^{-13}$ (5.3)	$8.70 \times 10^{-13}$
S5 0615+820	0.71	5.27	<0.8	$1.61 \pm 0.59$	$1.22 \times 10^{-13}$ (1.22)	$2.80 \times 10^{-13}$
1458+718	0.905	2.33	$1.2 \pm 0.2$	$1.44 \pm 0.04$	$8.02 \times 10^{-13}$ (10.8)	$2.24 \times 10^{-12}$
1328+254	1.055	1.08	$2.2 \pm 0.2$	$1.88 \pm 0.50$	$2.54 \times 10^{-13}$ (3.9)	$4.01 \times 10^{-13}$
1127–45	1.187	4.09	$3.3 \pm 0.2$	$1.24 \pm 0.03$	$1.25 \times 10^{-12}$ (2.17)	$5.74 \times 10^{-12}$
1245–197	1.28	4.72	<3.6	$1.47 \pm 0.02$	$2.50 \times 10^{-14}$	$6.60 \times 10^{-14}$
1416+067	1.439	2.50	$4.5 \pm 0.3$	$1.82 \pm 0.03$	$1.45 \times 10^{-12}$ (2.8)	$2.88 \times 10^{-12}$
1143–245	1.95	5.22	$9.4 \pm 5.2$	$1.75 \pm 0.39$	$1.10 \times 10^{-13}$ (19.6)	$2.30 \times 10^{-13}$

Absorbed power law model:  $A \times E^{-\Gamma} \times \exp(-N_{\text{H}} \sigma(E) - N_{\text{H}}^{\text{zabs}} \sigma(E(1 + z_{\text{abs}})))$  photons  $\text{cm}^{-2} \text{ s}^{-1} \text{ keV}^{-1}$ , where  $A$  is the normalization at 1 keV.  $\sigma(E)$  and  $\sigma(E(1 + z_{\text{abs}}))$  are the absorption cross sections (Morrison & McCammon 1983; Wilms, Allen & McCray 2000).

<sup>a</sup>  $N_{\text{H}}$  — equivalent galactic hydrogen column density.

<sup>b</sup>  $N_{\text{H}}^{\text{zabs}}$  — equivalent hydrogen column density of the absorber at the redshift of the source.

<sup>c</sup>  $\Gamma$  — X-ray photon index.

<sup>d</sup> Unabsorbed flux is shown in brackets.

to be easily detected in the radio? Can we detect extended emission in X-rays, and are GPS quasars simply extended radio sources, the core of which is boosted towards us?

In order to address these questions we selected a sample for the first systematic X-ray study of GPS/CSS sources using the following criteria:

- (1) Radio size >2 arcsec.
- (2) Redshift <2.
- (3) Low galactic hydrogen column.

We have obtained deep observations of sources with pre-existing X-ray measurements. For sources with no previous X-ray observations we requested short 5 ksec exposures in order to estimate their X-ray count rates and luminosity.

### 3.1 First Results from the Chandra Survey

Thus far we have observed 10 out of 14 sources (Table 1). The sample properties are presented in Figure 3. The details of the data analysis carried out with CIAO 2.2 software will be presented elsewhere (Siemiginowska et al. in preparation). Here we summarise our main results.

All targeted sources were detected and their 0.1–2 keV fluxes found to be in the range of  $\sim 0.1\text{--}2.8 \times 10^{-12} \text{ erg cm}^{-2} \text{ s}^{-1}$ . We found an intrinsic absorption column in excess of the galactic column in six sources:  $N_{\text{H}} \sim 10^{21}\text{--}10^{22} \text{ cm}^{-2}$ . We can obtain a lower limit on the density of the absorber assuming that it provides the confinement within  $\sim 10 \text{ kpc}$  from the center. This gives a density of  $0.03\text{--}0.3 \text{ cm}^{-3}$ , compared to the average density

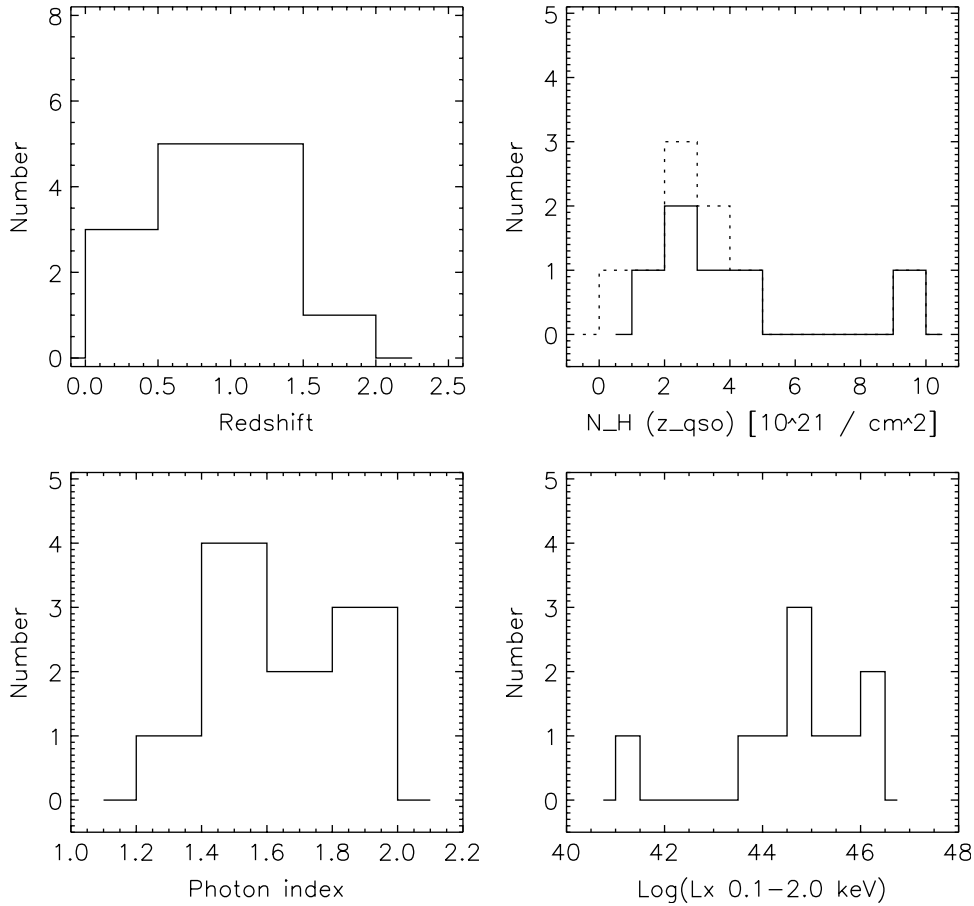


**Figure 3** The *Chandra* GPS/CSS sample. Top left: Redshift distribution. Top right: Distribution of the equivalent hydrogen column density in excess of the galactic column for the sample. Dashed line indicates sources with upper limits. Bottom left: Distribution of photon index within the sample. Bottom right: Rest frame luminosity within 0.1–2 keV. The GPS galaxy has the lowest X-ray luminosity in this plot.

of  $1\text{--}10 \text{ cm}^{-3}$  required to permanently confine a jet in the numerical simulations of De Young (1993).

#### 4 Summary

We have discovered X-ray jets in two GPS quasars. The jets travel up to several hundred kpc from the active nucleus. Our observations are compatible with the intermittent activity model, in which old electrons ( $\gamma \sim 10^3$ ) from previous activity are detectable in X-rays, via CMB Comptonization (LOFAR<sup>1</sup> may detect them directly), while new components expand into the medium formed by the previous active phase. However, six out of ten GPS sources show intrinsic absorption columns:  $N_H > 10^{21} \text{ cm}^{-2} \Rightarrow n_e > 0.03\text{--}0.3 \text{ cm}^{-3}$  suggesting that the sources could be both confined and intermittent.

Alternatively GPS quasars may simply be extended radio sources with the core boosted towards us (see Stanghellini 2003).

#### Acknowledgments

This research is funded in part by NASA contracts NAS8-39073. Partial support for this work was provided by the National Aeronautics and Space Administration through Chandra Award Number GO-01164X and GO2-3148A issued by the Chandra X-Ray Observatory Center, which is operated by the Smithsonian Astrophysical Observatory for and on behalf of NASA under contract NAS8-39073.

#### References

- Antonelli, L. A., & Fiore, F. 1997, *Mem della Soc Astron Ital*, 68, p. 299
- Bechtold, J., Siemiginowska, A., Aldcroft, T. L., Elvis, M., & Dobrzycki, A. 2002, *ApJ*, 562, 133
- Elvis, M., Fiore, F., Wilkes, B., McDowell, J., & Bechtold, J. 1994, *ApJ* 422, 60
- De Young, & David, S. 1993, *ApJ*, 402, 95
- Harris, D. E., & Krawczynski, H. 2002, *ApJ*, 565, 244
- Lane, W., Briggs, F. H., & Smette, A. 2000, *ApJ*, 532, 146
- Morrison, R., & McCammon, D. 1983, *ApJ*, 270, 119
- O’Dea, C. P. 1998, *PASP*, 110, 493

<sup>1</sup>Low frequency array, see [www.lofar.org](http://www.lofar.org)

- O'Dea, C. P., De Vries, W. H., Worrall, D. M., Baum, S. A., & Koekemoer, A. 2000, *AJ*, 119, 478
- Rao, S. M., & Turnshek, D. A. 1998, *ApJ*, 500, L115
- Siemiginowska, A., Bechtold, J., Aldcroft, T. L., Elvis, M., Harris, D. E., & Dobrzycki, A. 2002a, *ApJ*, 570, 543
- Siemiginowska, A., et al. 2002b, *ApJ*, submitted
- Stanghellini, C., O'Dea, C. P., Dallacasa, D., Baum, S. A., Fanti, R., & Fanti, C. 1998, *A&AS*, 131, 303
- Stanghellini, C. 2003, *PASA*, 20
- Wilms, J., Allen, A., & McCray, R. 2000, *ApJ*, 542, 914